

Dynamic plowing nanolithography on polymethylmethacrylate using an atomic force microscope

M. Heyde and K. Rademann

Humboldt-University, Institute of Physical and Theoretical Chemistry, Bunsenstr. 1, D-10117 Berlin, Germany

B. Cappella,^{a)} M. Geuss, and H. Sturm

Federal Institute of Materials Research (BAM), Lab. VI.32, Unter den Eichen 87, D-12200 Berlin, Germany

T. Spangenberg and H. Niehus

Humboldt-University, Institute of Physics, Invalidenstr. 110, D-10115 Berlin, Germany

(Received 13 June 2000; accepted for publication 19 September 2000)

We present dynamic plowing nanolithography on polymethylmethacrylate films, performed with a scan-linearized atomic force microscope able to scan up to 250 μm with high resolution. Modifications of the surface are obtained by plastically indenting the film surface with a vibrating tip. By changing the oscillation amplitude of the cantilever, i.e., the indentation depth, surfaces can be either imaged or modified. A program devoted to the control of the scanning process is also presented. The software basically converts the gray scale of pixel images into voltages used to control the dither piezo driving cantilever oscillations. The advantages of our experimental setup and the dependence of lithography efficiency on scanning parameters are discussed. Some insights into the process of surface modifications are presented. © 2001 American Institute of Physics. [DOI: 10.1063/1.1326053]

I. INTRODUCTION

In the last few years there has been a considerable interest in proximal-probe nanolithography, i.e., methods aimed to modify surfaces by means of a scanning tunneling microscope or an atomic force microscope (AFM). The AFM has already successfully been employed to pattern Si,¹⁻³ GaAs⁴ or resist⁵ by inducing a local anodic oxidation of the sample surface.

A number of additional works take advantage of the possibility of directly machining the sample surface by means of AFM cantilever tips. This can be achieved in two ways, called *static* and *dynamic plowing*. In the static plowing⁶⁻⁹ the AFM is employed in contact mode to pattern a single resist layer and subsequently use it as an etch mask. This technique, while being a low-cost and low-effort technique, presents some drawbacks. It has been proved that, while cutting a furrow into the resist by static plowing, torsion of the cantilever may lead to edge irregularities.¹⁰ Additionally, depending on the local stiffness of the sample, while imaging the surface before or after the modification, further modifications may occur due to dragging of the surface.

By dynamic plowing lithography (DPL)¹¹⁻¹⁴ the surface is modified by indenting it with a vibrating tip in the AFM tapping mode. This method provides a lithography technique that is nearly free from problems due to cantilever torsion and permits us to image the modified surface without any further modification. Despite the great advantages of this technique, little work has been done to understand its principles and to improve the performances.

In this article we present the results obtained on polymethylmethacrylate (PMMA) films, which are often employed as resist films in etching lithography, taking advantage of a scan-linearized microscope controlled by an ADwin-Gold system. These results provide some insights in the basic process of the lithography and suggest a choice of scanning parameters likely to improve the efficiency of the technique.

In Sec. II, we present the microscope and the program devoted to dynamic plowing lithography; in Sec. III we describe the technique and discuss the dependence of lithography efficiency on scanning parameters, showing some results on PMMA films.

II. EXPERIMENTAL SETUP

The AFM used in our experiments is made up of a commercial microscope head (Topometrix TMX 2000 Explorer, Santa Clara, CA), a piezoelectric scanning table (P-517.2CL, Physik Instrumente GmbH & Co., Waldbronn, Germany) for XY scanning, and a Z piezo (P-753.11C, Physik Instrumente GmbH and Co., Waldbronn, Germany) for Z positioning. Both the PI table and the PI Z piezo are equipped with integrated capacitive displacement sensors. The maximum scan range of the scanning table is $250 \times 250 \mu\text{m}^2$. The maximum Z range is 12 μm .

A schematic representation of the experimental setup is given in Fig. 1. The electronic control unit is realized with an ADwin-GOLD system (Keithley Instruments, Inc., Cleveland, OH). The ADwin-Gold system consists of a digital signal processor (DSP), a local memory of 4 MB, 16 analog inputs, 8 analog outputs, 32 digital I/O lines, and a trigger input. The power supply of the ADwin-Gold system is independent of the PC; this feature permits it to have a better S/N

^{a)}Electronic mail: brunevo.cappella@gmx.de

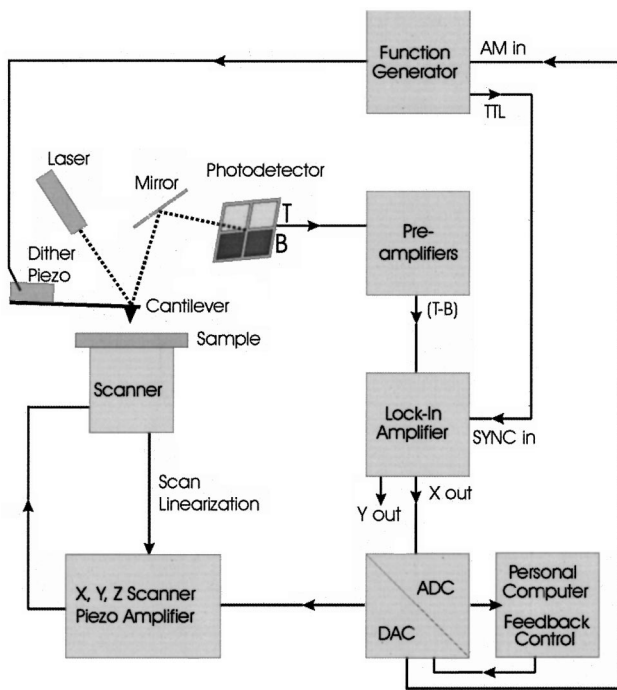


FIG. 1. Schematic representation of the experimental setup employed in DPL experiments.

ratio. The ADwin-Gold CPU processor is an Analog Devices-SHARC DSP that handles system management, data acquisition, online processing, and control of outputs. It additionally handles the communication between the ADwin system and a PC (Pentium Type Class) via a serial link (10 Mbit/s). Using a dedicated processor, data processing of each measurement can take place immediately after acquisition with a sample rate of about 100 kHz.

The real-time development tool ADbasic allows programming of mathematical operations and functions, which are executed on the DSP immediately after each sampling step. The software and hardware permit us to operate the microscope in several modes, e.g., contact mode, non-contact mode, tapping mode, etc. The user interface has been written in Borland Delphi (Borland Inprise Corporation, Scotts Valley, CA) for Object Windows. Thanks to the flexibility of the system, we have the possibility to add nearly every desired scanning mode. Even imaging modes that need a second feedback circuit, like force-modulation, Kelvin force microscopy,¹⁵ or constant dynamic indentation modes,¹⁶ can be performed. Also adhesion modes,¹⁷ in which a force-distance curve is acquired on every pixel of the scanned area, or other types of imaging point spectroscopy modes, can be performed.

In this article we will focus on the nanolithography mode based on tapping mode. When the microscope is operated in tapping mode, the cantilever driven by a dither piezo vibrates near its resonance frequency. The oscillation amplitude depends on the distance between cantilever and sample. A feedback loop keeps the vibration amplitude constant by changing the extension of the Z piezo, and hence the distance between the sample surface and the cantilever. The topography of the sample is reconstructed from the changes of the Z piezo extension. In conventional tapping mode the amplitude

of the oscillations is chosen so that the tip of the cantilever gently taps the sample surface. In dynamic plowing lithography, modifications of the sample can be obtained by changing the modulation amplitude applied to the dither piezo that drives the cantilever oscillations. By increasing the oscillation amplitude the sample is further approached to the tip. As the tip is likely to indent the sample surface, elastic and plastic deformations are obtained. The oscillation amplitude is changed by means of one of the analog outputs of the electronic control unit driving the amplitude modulation (AM) input of the function generator that controls the voltage given to the dither piezo. The analog output permits us to perform lithography techniques based on electrochemistry (switching dc, ac, or pulsed voltages applied to conductive tips and levers) or on nanomechanics (set point change, in contact or in tapping mode). All the experiments presented in this article have been performed by changing the amplitude during tapping mode imaging.

Dynamic plowing lithography can be performed in a vector scan mode or in an image pattern scan mode. In the vector scan mode, the software provides a set of commands that permit us to write lines of arbitrary length and direction with defined scan speed and oscillation amplitude.

The image pattern scan mode, which has been used in all the experiments presented in this article, is a synchronization of the raster scan mode with the desired pattern. The pattern can be constructed with a simple pixel-oriented paint program. Afterwards, the pattern is converted to the self-made pattern file format. The oscillation amplitude values are given by a 16 bit resolution mask which can be additionally split using a look-up table. In our experiments the writing of nanostructures was performed with a 1 bit mask.

The signal used to write, V_w , is a 20-fold factor larger than the signal used to read, V_r . Thus, when the cantilever is far from the surface, the writing free oscillation amplitude, A_{wf} , is a 20-fold factor larger than the reading free oscillation amplitude, A_{rf} . The efficiency of the writing process, i.e., the depth of the written structures, depends on the difference $A_w - A_r$, where A_w and A_r are the writing and reading amplitudes when the tip is close to surface. This depends on $A_{wf} - A_{rf}$, but also on the damping of the cantilever oscillations due to the interactions between the cantilever and the sample. The damping depends in turn on the set-point amplitude.

A_{rf} is typically about 120 nm. The oscillation amplitude in tapping mode feedback can be deduced, with a relatively large uncertainty,^{18,19} from the percentage set-point value. The effective amplitude during writing depends on the damping, which depends in turn on the set-point. Further, the complicated interplay between lithography and feedback loop (see below) makes it impossible to estimate the oscillation amplitude.

By using a typical tapping mode cantilever, it is possible to indent a surface and immediately image the indentation, taking advantage of the backward scanning image. This *in situ* imaging ability eliminates the need to move the sample, to change tips, to relocate the area for scanning, or to use an entirely different instrument to image the indentation. In tapping mode, it is still possible to image soft samples with

relatively low forces using cantilevers with higher spring constants.

The PMMA films have been prepared by depositing a solution of 0.4 g of PMMA in 10 ml of tetrahydrofuran (THF) on a glass slide and letting the THF slowly evaporate within 24 h. Both the glass and the air side of the film are quite flat, but only the glass side has been used in the experiments reported here. The film thickness is about 1 μm . The mean roughness of the glass side of the film, calculated as the arithmetic mean of the deviations in height from the profile mean value, has been evaluated to 8 \AA in an image of $5 \times 5 \mu\text{m}^2$.

Commercially available cantilevers (Pointprobe NCL-50, Nanosensors, Wetzlar-Blankenfeld, Germany) with length $L=225 \mu\text{m}$, width $W=38 \mu\text{m}$, thickness $T=7 \mu\text{m}$, resonance frequency $F=156 \text{kHz}$, and spring constant $K=31-71 \text{N/m}$ were used. All experiments were performed at room temperature in air.

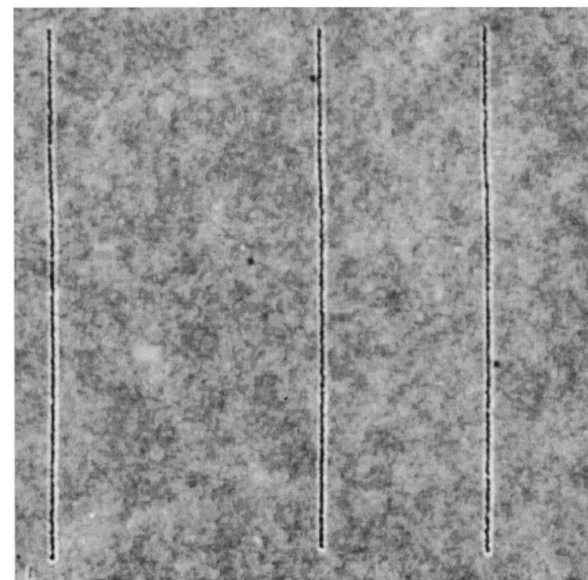
The tip of the cantilever is not damaged during lithography, and no adsorption of polymer occurs. We have employed the same cantilever for more than 50 lithography experiments. We have not seen, during the imaging phase, any changes in the tip structure and form.

III. EXPERIMENTAL RESULTS AND DISCUSSION

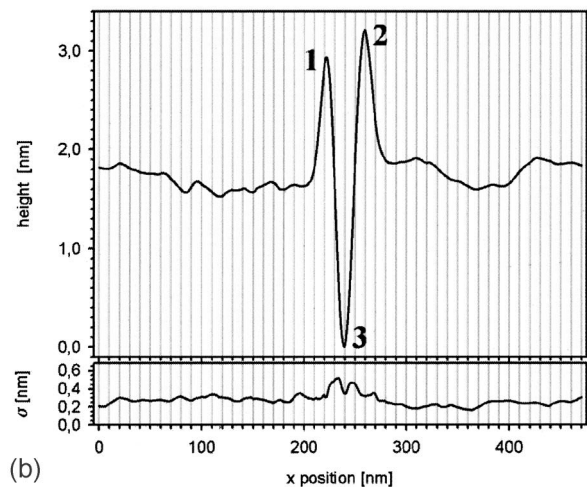
We have performed dynamic plowing lithography on PMMA films. Figure 2(a) shows three lines written on PMMA. The lines are $2.7 \mu\text{m}$ long. Thanks to the scan-linearized system, we were able to write straight lines with a length up to $50 \mu\text{m}$. The shape of the lines can be observed in Fig. 2(b). The tip embosses a groove and the carved PMMA accumulates on the sides of the groove. The width of the three lines, i.e., the X distance between the points 1 and 2, is $40 \pm 3 \text{ nm}$, $38 \pm 4 \text{ nm}$, and $37 \pm 2 \text{ nm}$, respectively. The width is likely to depend on the shape and dimensions of the tip. With sharper tips we could obtain 30 nm wide lines. The depth of the three lines, i.e., the Z distance between point 3 and the highest between the points 1 and 2, is $3.4 \pm 0.4 \text{ nm}$, $3.4 \pm 0.3 \text{ nm}$, and $3.4 \pm 0.3 \text{ nm}$.

The shape of the written line is not always the same. Depending on the direction of scanning (with respect to the axis of the cantilever), the carved material may be accumulated either on both sides or only on one side (left or right). The depth of the written line depends of course on the difference $A_w - A_r$, but it depends also on the direction of the line with respect to the fast scan direction. If the fast scan direction is conventionally assumed to be the X direction, horizontal lines are less deep than vertical lines written with the same $A_w - A_r$. Sometimes horizontal lines cannot be written at all.

Figure 3(a) shows a PMMA surface modified, with a mask made up of vertical stripes instead of vertical lines. The scanning direction is from left to right. The two graphs of Fig. 3(b) show the Z profiles in two different regions (see below). It is evident that strong modifications occur only at the border of the stripes, and not inside the stripes. In particular, there is a groove at the beginning of each stripe (positions a-e) and a protruding line at the end of each stripe



(a)



(b)

FIG. 2. (a) Topography of lines written in PMMA (tapping mode image, $3 \times 3 \mu\text{m}^2$, $\Delta Z=4.8 \text{ nm}$). (b) Z profile of a line averaged over 100 scan lines with line-to-line distance 5 nm , and standard deviation σ .

(positions $\alpha-\epsilon$). Inside the stripes the surface is much more irregular and, on an average, higher than outside the stripes, i.e., in the unmodified region. The position of the groove and of the protruding line depends again on the scanning direction. In a similar image, but written from right to left, both the groove and the protruding line are close one to the other at the beginning of the stripe. In the first case the carved material is accumulated to the right and carried to the end of the stripe by the scanning tip. Also in the second case the carved material is accumulated to the right, but not carried to the end of the stripe, because the tip is scanning from the right to the left.

In a certain sense, the system reacts mainly at the border of the structure to be written, or, in other words, it reacts mainly to the first derivative of the lithography signal. In the surface of Fig. 3(a), four different regions can be seen. The regions from the beginning to line 1, and from line 2 to line 3, have been written with a set-point amplitude of 44% of the free resonance amplitude; the regions between lines 1 and 2

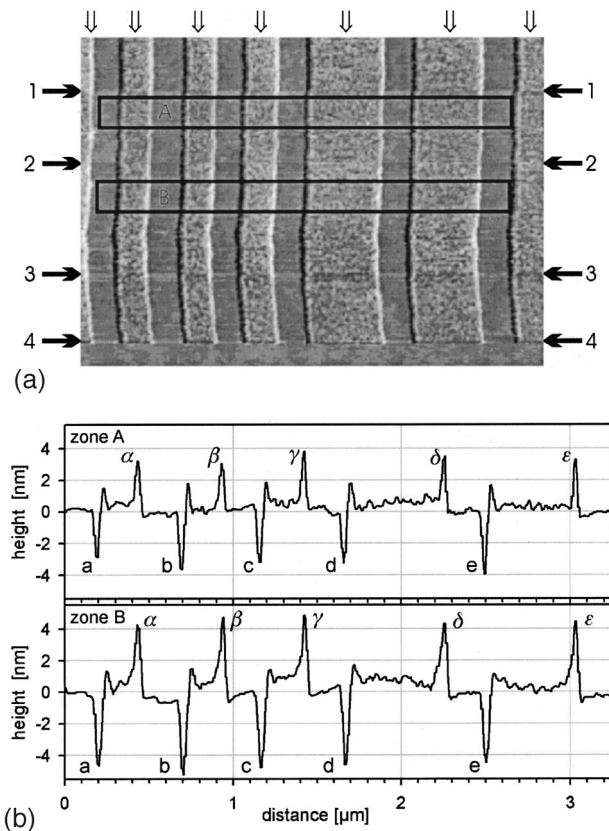


FIG. 3. (a) Tapping mode topography image after DPL on PMMA performed with two different set-point amplitudes (Top-“1”: 44%; “1”-“2”: 15%; “2”-“3”: 44%; “3”-“4”: 15%; “4”-end: DPL off). The arrows indicate the positions of the stripes. The rectangles A and B indicate the position for line analysis (b). (Tapping mode image, $3.63 \times 2.59 \mu\text{m}^2$, $\Delta Z = 11.9 \text{ nm}$.) (b) Line analysis of a weak and a strong DPL (15% and 44% set-point amplitude, respectively); average of 27 scan lines each; top: zone A, bottom: zone B. The stripes are not straight because of the changes of the set-point that induce problems in the scan linearization system.

and from line 3 to the end have been written with a set-point amplitude of 15%. The mean difference of height between the groove and the protruding line is $9.8 \pm 1.0 \text{ nm}$ in the first and third regions and $7 \pm 1 \text{ nm}$ in the second and fourth regions. The efficiency of the lithography, i.e., the depth of the written lines, increases with increasing set-point amplitude, i.e., with increasing distance between the tip and the surface. This has been confirmed with the lines shown in Fig. 4(a). The set-point amplitude has been changed linearly from 15% to 45% while writing the lines. Figure 4(b) shows the dependence of the depth on the set-point amplitude for the central line.

Such a dependence of the depth of the written structures on the set-point amplitude can be understood by analysis of the following signals acquired during the writing procedure by means of an oscilloscope (Fig. 5):

- (a) the complete cantilever deflection signal, $(T-B)_{\text{dyn}}$, calculated by subtracting top and bottom photodetector intensity;
- (b) the low-pass-filtered component of the cantilever deflection signal, $(T-B)_{\text{stat}}$;
- (c) the real part of the lock-in amplifier output signal (X signal), i.e., the feedback signal used in our experiments;

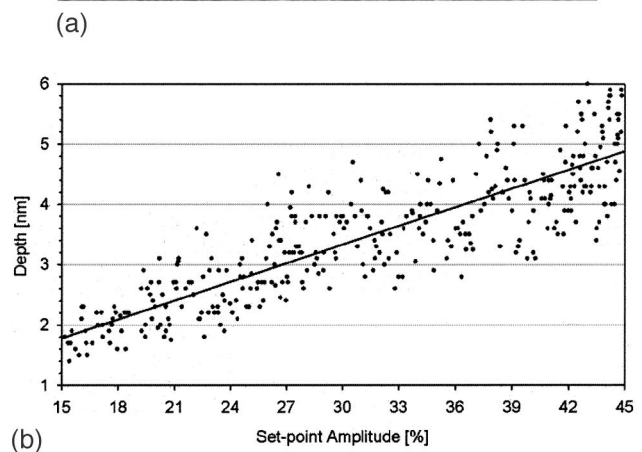
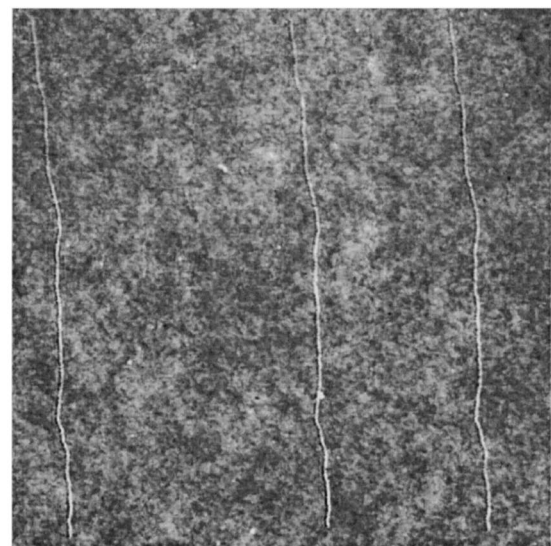


FIG. 4. (a) Tapping mode topography image of three lines written with increasing set-point amplitude (from 15% to 44%). Image size $7.3 \times 7.3 \mu\text{m}^2$, $\Delta Z = 3.9 \text{ nm}$. The lines are not straight because of the changes of the set-point that induce problems in the scan linearization system. (b) Set-point dependence of the line depth, showing a linear relationship.

- (d) the imaginary part of the lock-in amplifier output signal (Y signal); and
- (e) the driving signal given to the Z piezo, i.e., the response of the feedback loop.

The signals shown in Fig. 5 correspond to the beginning of a stripe. At the beginning of the writing signal, as soon as V_r is changed to V_w , some oscillations in both the static and the dynamic component of $T-B$ are evident. Peaks in the $(T-B)_{\text{stat}}$ signal show that the cantilever approaches to and withdraws from the sample. Accordingly, the oscillation amplitude decreases or increases. In particular, at the very beginning of the stripe, the oscillation increases and the tip approaches to the sample. This large change in the amplitude affects but little the X signal (only a slight increase can be seen, marked with an arrow), while there is a large peak in the Y signal. Hence, the feedback signal does not react to this first peak, and “sees” only the subsequent ones. After the first increase, the amplitude decreases, because the tip is close to the sample. Also the X signal decreases, and the sample is withdrawn, in order to increase the oscillation am-

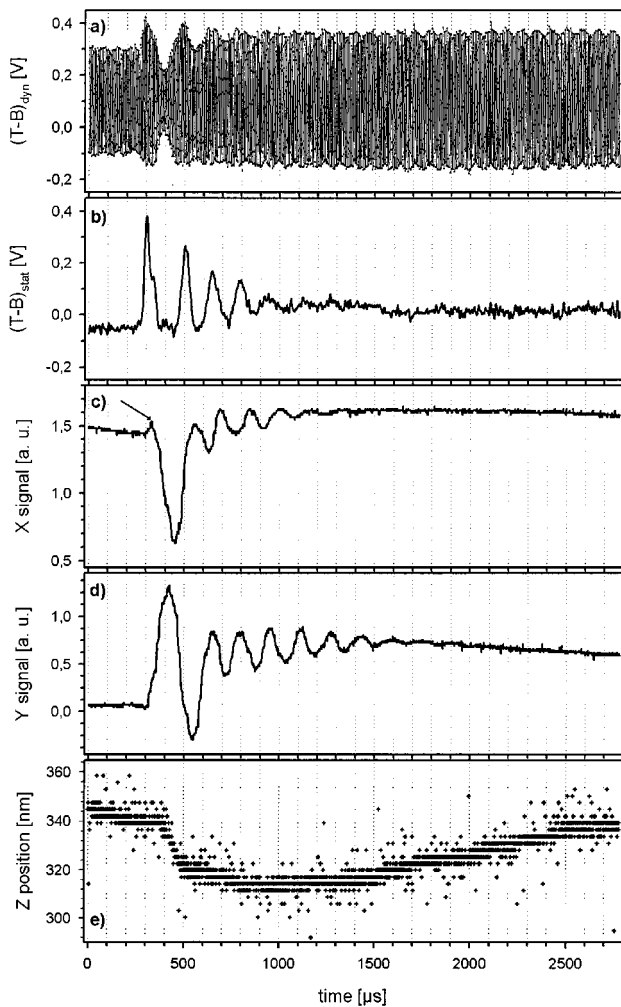


FIG. 5. From the top to the bottom: (a) Unfiltered cantilever deflection $(T-B)_{dyn}$ (set point 45%); (b) $(T-B)_{stat}$, low-pass filtered from $(T-B)_{dyn}$, a measure of the average position of the tip; (c) real part of $(T-B)_{dyn}$ (LIA output X signal); (d) imaginary part of $(T-B)_{dyn}$ (LIA output Y signal); and (e) Z piezo movement. The Z movement, damped by the feedback and bandwidth limited by the HV amplifier and its capacity, is restabilized after ≈ 2.4 ms.

plitude. Even if there are some peaks also in this region, the sample is too far away to be indented. Then the feedback signal slowly increases and the sample is approached, in order to reduce the oscillation amplitude (not to be seen in Fig. 5). Although the feedback loop is not able to reach the set-point, oscillations are greatly damped, and only a slight indentation can be achieved. As a matter of fact, the only moment in which oscillations increase and the sample is not withdrawn is the very first peak. Hence, deep indentation occurs only at the very beginning. This is confirmed by the Y signal, that, in a harmonic oscillator model, is an indicator of the energy loss. When the same signals are acquired for a free cantilever, at the beginning of the stripe, since the feedback is not active, the real part is free to increase and, except for an initial small increase, the imaginary part decreases. In the case of the free cantilever, all the energy is employed in increasing the oscillations and no energy is lost in indentation. In the case of the tip close to the sample, the first peak of the Y signal shows that a large part of the energy of the

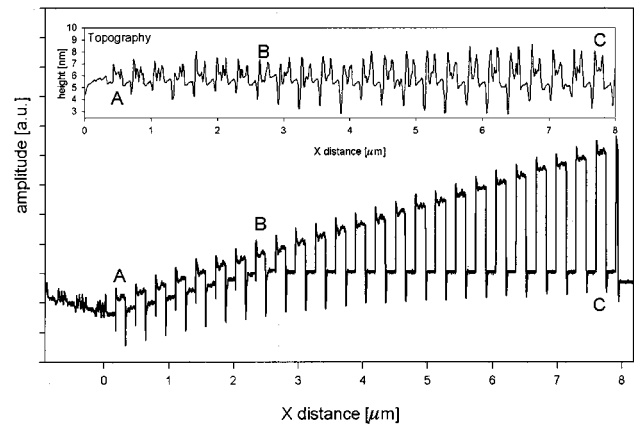


FIG. 6. Oscillation amplitude while writing a row of a stripe mask without feedback. The inset shows the Z profile of the modified surface. The row is $8 \mu\text{m}$ long.

oscillating cantilever is employed in indentation of the sample. Also in the following the Y signal is slightly larger than during the reading, due to the small indentation occurring inside the stripe.

This behavior of the feedback during writing explains why horizontal lines cannot be written. The feedback loop is antagonistic to the lithography process. Even if the oscillation amplitude is increased, the feedback loop is able to reduce it again by slowly approaching the sample to the cantilever. Only during the first large increase of oscillations is the tip close enough to the sample and able to indent it. The important factor for the efficiency of the lithography is the difference $A_w - A_r$, and not the difference $A_{wf} - A_{rf}$. The signals shown in Fig. 5 have been acquired for two different set-points, namely 15% and 45% (only the signals relative to a 45% set point are shown). The increase of A, and also the amplitude of the first peak, responsible for the writing, is actually larger for larger set-points. This explains the results shown in Figs. 3 and 4. Also, the proportional factor of the PID gain, P , has been changed. The stripes written with a small P are better than the stripes written with a large P . In the first case the difference between the grooves and the protruding lines is 7.6 ± 0.5 nm, in the second 4.6 ± 0.5 nm. Further, when the feedback is weak, not only the border of the stripe but also the region inside the stripe is written. The PID gain is actually so bad that the increased oscillations cannot be damped. Finally, the scan rate has been changed, but no differences are to be seen between stripes written with different scan rates.

Since lithography and the feedback loop are antagonists, the best efficiency of the lithography process can be achieved when writing without feedback. Figure 6 shows the oscillation amplitude while writing a row of a stripe mask. The inset shows the Z profile of the modified surface. The row, going from A to C, can be divided in two regions: from A to B, and from B to C. In the first region, from A to B, both oscillation amplitudes A_w and A_r are damped, because the tip is close to the sample. Due to the tilt of the sample, the distance between the tip and sample increases, and in point B A_r reaches its maximum and is no more damped. A_w never reaches its maximum value and is always damped. As can be

seen in the inset, the damping of A_w and the relative small indentation depth for the first stripes (region A–B) lead to stripes written only at the border with a difference in height between the grooves and the protruding lines of about 5 nm. The stripes are better defined, and the difference in height increases up to about 9 nm, as A_w is less damped and the tip is able to indent the sample.

- ¹J. A. Dagata, J. Schneir, H. H. Harary, C. J. Evans, M. T. Postek, and J. Bennett, *Appl. Phys. Lett.* **56**, 2001 (1990).
- ²J. Servat, P. Gorostiza, F. Sanz, F. Pérez-Murano, N. Barniol, G. Abadal, and X. Aymerich, *J. Vac. Sci. Technol. A* **14**, 1208 (1996).
- ³R. Garcia, M. Calleja, and F. Pérez-Murano, *Appl. Phys. Lett.* **72**, 2295 (1998).
- ⁴M. Ishii and K. Matsumoto, *Jpn. J. Appl. Phys., Part 1* **34**, 1329 (1995).
- ⁵K. Wilder, C. F. Quate, D. Adderton, R. Bernstein, and V. Elings, *Appl. Phys. Lett.* **73**, 2527 (1998).
- ⁶M. Wendel, S. Kühn, H. Lorenz, J. P. Kotthaus, and M. Holland, *Appl. Phys. Lett.* **65**, 1775 (1994).
- ⁷P. Pingue, M. Lazzarino, F. Beltram, C. Cecconi, P. Baschieri, C. Frediani, and C. Ascoli, *J. Vac. Sci. Technol. B* **15**, 1398 (1997).
- ⁸R. Magno and B. R. Bennett, *Appl. Phys. Lett.* **70**, 1855 (1997).
- ⁹S. Miyake, *Appl. Phys. Lett.* **67**, 2925 (1995).
- ¹⁰V. Bouchiat and D. Esteve, *Appl. Phys. Lett.* **69**, 3098 (1996).
- ¹¹B. Klehn and U. Kunze, *J. Appl. Phys.* **85**, 3897 (1999).
- ¹²M. Wendel, S. Kühn, H. Lorenz, J. P. Kotthaus, and M. Holland, *Appl. Phys. Lett.* **65**, 1775 (1994).
- ¹³S. Skaberna, M. Versen, B. Klehn, U. Kunze, D. Reuter, and A. D. Weck, *Ultramicroscopy* **82**, 153 (2000).
- ¹⁴M. Wendel, H. Lorenz, and J. P. Kotthaus, *Appl. Phys. Lett.* **67**, 3732 (1995).
- ¹⁵M. Nonnenmacher, M. P. O'Boyle, and H. K. Wickramasinghe, *Appl. Phys. Lett.* **58**, 2921 (1991).
- ¹⁶M. Munz, H. Sturm, E. Schulz, and G. Hinrichsen, *Composites* **29A**, 1251 (1998).
- ¹⁷B. Cappella, P. Baschieri, C. Frediani, P. Miccoli, and C. Ascoli, *Nanotechnology* **8**, 82 (1997).
- ¹⁸B. Anczykowski, D. Krüger, and H. Fuchs, *Phys. Rev. B* **53**, 15485 (1996).
- ¹⁹A. Kühle, A. H. Sørensen, and J. Bohr, *J. Appl. Phys.* **81**, 6562 (1997).